3rd EUROPEAN CONFERENCE ON
EARTHQUAKE ENGINEERING & SEISMOLOGY
BUCHAREST, ROMANIA, 2022

Seismic fragility assessment of two low-rise equipment-supporting RC industrial buildings

A. K. Kazantzi – Resilience Guard GmbH, Switzerland, e-mail: nancy.kazantzi@resilienceguard.ch

N. D. Karaferis – National Technical University of Athens, Greece, e-mail: nkaraferis@mail.ntua.gr

V. E. Melissianos – National Technical University of Athens, Greece, e-mail: melissia@mail.ntua.gr

K. Bakalis – École Polytechnique Fédérale de Lausanne, Switzerland, e-mail: konstantinos.bakalis@epfl.ch

D. Vamvatsikos – National Technical University of Athens, Greece, e-mail: divamva@mail.ntua.gr

Abstract: Open-frame reinforced concrete (RC) buildings for supporting essential mechanical/electrical equipment are encountered in almost all industrial plants. Hence, to ensure the undisrupted operation of an industrial facility, the integrity of such structural assets along with their nested nonstructural components should be verified against a spectrum of natural and man-made hazards. Focusing on the earthquake peril, this study presents an analytical seismic fragility assessment framework for two RC equipment-supporting buildings that are deemed typical to an oil refinery. The proposed fully-probabilistic fragility concept, utilises reduced-order building models for the evaluation of the induced seismic demands and accounts for both drift and acceleration-sensitive failure modes in the definition of the damage states. The findings can be exploited by designers and facility managers for developing efficient pre- and post-event risk-aware mitigation/response strategies and are delivered in a manner that can be readily integrated into the seismic performance assessment framework of an entire industrial facility.

Keywords: seismic fragility, industrial building, critical infrastructure, oil refinery

1. Introduction

Assessing the seismic performance of critical industrial facilities in modern industrialised countries is a topic of paramount importance, since the impact of a potential failure incident to any of their structural and nonstructural assets could result to direct (e.g., fires or uncontrolled leakage) as well as to indirect (e.g., severe service disruptions) losses (Kiremidjian et al, 1985). Among the most critical industrial facilities, are the oil refineries, due to their key role in the fossil fuel production chain as well as due to the significant amount of hazardous materials that are being processed. Their importance is acknowledged in the design codes, which, in an attempt to secure their seismic structural and operational integrity, enforce strict design criteria integrated within a prescriptive intensity-based design framework (e.g., Kazantzi and Vamvatsikos, 2021). Yet, despite the conservatism that is imposed in the design process, natural-technological (NaTech) accidents are still triggered to such facilities by earthquake events (e.g., Hatayama, 2008; Krausmann and Cruz, 2021). This, essentially demonstrates that counting on an implicit risk-aware framework to deliver seismic integrity allows room for a nonnegligible failure potential that needs to be quantified by means of a seismic fragility assessment and then appropriately catered.

Up until now, research on the seismic fragility of oil refinery structures is unevenly distributed among them. Hence, while some of them, such as the liquid storage tanks, the pipe-racks and the pressure vessels are considered well-studied (e.g., Patkas and Karamanos, 2007; Bakalis et al, 2017; Vathi et al, 2017; Di Sarno and Karagiannakis, 2020), others, such

as the flare stacks, chimneys, piping and open-frame structures, have received comparatively less attention. Owing to the above, this study is built upon an analytical context for deriving seismic fragility curves for two low-rise industrial building-type assets, with structural configurations typical to an oil refinery, supporting several types of industrial equipment. Seismic damages are accounted for both the supporting structure as well as its nonstructural components, including nested acceleration-sensitive industrial equipment and other drift-sensitive attachments.

2. Case study open-frame equipment-supporting buildings

Two reinforced concrete (RC) moment-resisting frames, namely RC1–2 as illustrated in Fig. 1, are considered in the present work. The process equipment that are nested to each one of these open-frame structures is detailed in Table 1. From a structural point of view, the considered buildings are overdesigned as it is typically the case for the structures serving an industrial facility. Hence, little (if any) structural damage is anticipated even during strong ground shaking, under the assumption that appropriate routine maintenance is exercised throughout their life cycle. Regarding the process equipment, each is assigned to an importance category (IC) class in view of its failure impact on the refinery process. Hence, IC I denotes equipment of low importance (i.e. marginally no disruption in case of failure), IC II denotes equipment of moderate importance (i.e. limited disruption in case of failure) and IC III denotes equipment of high importance (i.e. severe disruption in case of failure).

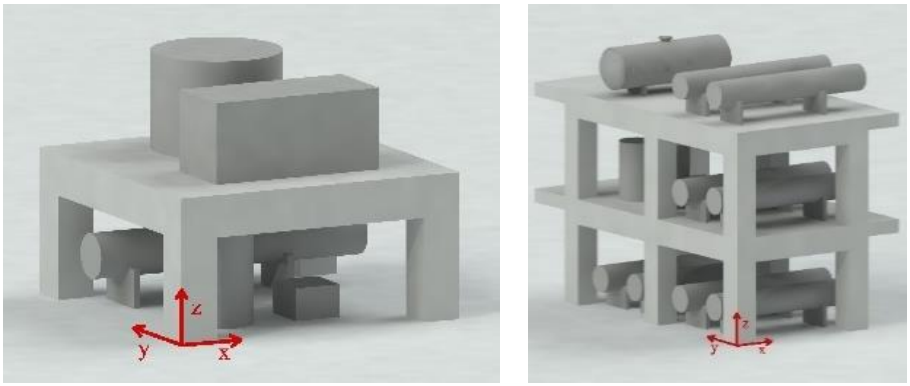

(a) RC1 (b) RC2

Fig. 1 - 3D representation of (a) the 1-storey and (b) the 2-storey RC buildings along with their nested process equipment.

Table 1. Nested equipment items per case study building with global axis designations per Fig. 1

Building ID	Elevation (m)	Item	Vibration period range		OS		IC
			$T_{comp,x}$(sec)	$T_{comp,y}$(sec)	x	y	
RC1	±0.0	Pump	0.10	0.10	1.10	1.10	II
T_x = 0.08sec		Vessel	0.10 – 0.20	0.10 – 0.20	1.20	1.20	I
T_y = 0.08sec		Heat exchanger	0.30 – 0.50	0.10 – 0.20	1.20	1.50	III
	+4.5	Vessel	0.10 – 0.20	0.10 – 0.20	1.20	1.20	I
		Vacuum charge	0.10 – 0.20	0.10 – 0.20	1.50	1.50	II
RC2	±0.0	4 × Heat exchanger	0.30 – 0.50	0.10 – 0.20	1.20	1.50	III
T_x = 0.21sec	+5.5	2 × Heat exchanger	0.30 – 0.50	0.10 – 0.20	1.20	1.50	III
T_y = 0.20sec		2 × Vessel	0.10 – 0.20	0.10 – 0.20	1.20	1.20	I
		2 × Pump	0.10	0.10	1.10	1.10	II
	+11.0	2 × Heat exchanger	0.30 – 0.50	0.10 – 0.20	1.20	1.50	III
		Horiz. vessel	0.30 – 0.50	0.10 – 0.20	1.20	1.50	II

Reduced-order building models were developed for evaluating the seismic response of the aforementioned buildings, in an attempt to balance the accuracy and the needed computational efficiency for practical fragility applications. Given the high-strength low-ductility design of the overdesigned structures, the two buildings were modelled in 3D using elastic beam-column elements in the OpenSees platform (McKenna and Fenves, 2001). The nonstructural components (equipment items) were not explicitly modelled. Instead, they were introduced to the building models as point masses only.

3. Definition of Damage States

For characterising the damage induced in the structural elements and the drift-sensitive nonstructural components attached to the building, a set of Damage States (DSs) was defined and the DSs were paired with specific maximum (over time and height) Interstorey Drift Ratio (IDR) Limit-State (LS) thresholds. Hence, DS1, associated with low damage, is assigned an IDR of 1%, as specified by EN1998-1 (CEN, 2004) for buildings without partition walls. DS2, associated with moderate damage, was paired to a threshold of 2% to account, among others, for any damage that is likely to occur in the vertical piping spanning across different storeys. The near-collapse DS3 is associated with a 4% IDR threshold.

The same set of DSs was also utilised to characterise the damage in the nested acceleration-sensitive nonstructural components (Table 1). In this case, the DSs were associated with damage that is likely to occur primarily in the component anchorage system, assuming the component itself does not fail earlier. The first failure of an IC I/II/II component, determined by the exceedance of its anchorage capacity, signifies the attainment of DS1/DS2/DS3, respectively, as per the description provided in Table 2.

Table 2. Building DS classification and associated LS definitions

DS	LS threshold	
	Drift-sensitive structural and nonstructural components	**Acceleration-sensitive nonstructural components**
DS1	$IDR > 1\%$	Anchorage failure of at least one component of IC I
DS2	$IDR > 2\%$	Anchorage failure of at least one component of IC II
DS3	$IDR > 4\%$	Anchorage failure of at least one component of IC III

The anchorage capacity (in acceleration terms) of the acceleration-sensitive equipment was evaluated by Eq. (1), following Annex 4.3.5 of EN1998-1 (CEN, 2004) for estimating the design seismic coefficient, S_{ac}, for each component. It was assumed that the component: (a) is located at the top of the building (irrespectively of actual position to account for typical engineering conservatism), (b) was designed to behave elastically (i.e. component behaviour factor q_a =1.00), (c) has an overstrength factor (OS) as per Table 1 and (d) has an importance factor γ_a equal to 1.50 as proposed by EN1998-1 for tanks and vessels containing toxic or explosive substances.

$$S_{a_{cap}} = \frac{S_{ac}\gamma_a}{q_a} \cdot OS \cdot \mathrm{g} \quad (1)$$

where, g is the gravity acceleration.

The component capacity acceleration $S_{a_{cap}}$ was then compared to the demand acceleration $S_{a_{dem}}$ that was obtained for the above-ground supported components by amplifying the Peak Floor Acceleration (PFA) estimated at the anchorage points with the component

amplification factor a_p, following the methodology proposed by Kazantzi et al. (2020) to account for component dynamic characteristics:

$$S_{a_{dem}} = PFA \cdot a_p \quad (2)$$

The factor a_p essentially quantifies the ratio of elastic Peak Component Acceleration (*PCA*) over the *PFA*, accounting for the component damping and the non-trivial amplification of demands when the fundamental period of the nonstructural component is close to a predominant modal period of the supporting structure. The fundamental period of vibration of the nonstructural component in the direction of interest was taken equal to the median value of the period ranges reported in Table 1. For ground-level components, the component acceleration demands are represented by the pertinent ground spectral acceleration ordinates.

4. Seismic demand

Targeting a refinery-wide application, the fragility curves were assessed for two Intensity Measures (IMs), these being: (a) the asset-agnostic peak ground acceleration, PGA, a reference IM often used in fragility studies, and (b) the asset-aware spectral acceleration, averaged over a period range, $AvgS_a$ (e.g., Cordova et al, 2000; Tsantaki et al, 2017; Eads et al, 2015; Kazantzi and Vamvatsikos, 2015). Both IMs were evaluated in the geomean sense to comply with the majority of existing ground motion prediction equations. For *PGA*, this entails taking the geometric mean of the respective values recorded in the two horizontal directions. For $AvgS_a$, we employed geomean spectral acceleration ordinates for periods spanning 0.1sec to 1.0sec at 0.1sec intervals. A set of 30 "ordinary" non-pulse-like, non-long-duration natural ground motion records was employed to carry out the response time-history analyses. The records were selected by Bakalis et al. (2018) for the same definition of $AvgS_a$, using the conditional spectrum approach (Lin et al, 2013) to achieve hazard consistency with the considered site.

5. Seismic fragility assessment

Once the demand and capacity of the considered structures and their nested equipment have been evaluated, one may proceed to the fragility evaluation. Fragility curves constitute a key element in a seismic risk assessment since are used for quantifying the damage potential for the assets of interest. Thus, the probability of exceeding a specific LS, or equivalently the probability of being in a particular DS, is computed. The derivation of analytical fragility curves via response-history analyses has been demonstrated in several past studies (e.g., Dymiotis et al, 1999; Kwon and Elnashai 2006; Kazantzi et al, 2011). The fragility is essentially a function of the IM and may be expressed, under a typical lognormality assumption (Cornell et al, 2002), as:

$$P[D > C_{LS}|IM] = P[LS \text{ violated} \mid IM] = \Phi\left(\frac{\ln IM - \ln IM_{LS50}}{\beta_{LS}}\right) \quad (3)$$

where D is the EDP demand, C_{LS} is the EDP capacity threshold paired to a specific LS, IM_{LS50} is the median IM value required to violate a given EDP threshold after Table 2, and β_{LS} is the dispersion, equal to the standard deviation of the natural logarithm of the data.

The drift-sensitive fragilities were treated in a global sense, via the maximum IDR over all floors. On the other hand, given that acceleration-sensitive components govern the response, they received a component-specific treatment, accounting for demand and capacity on a component-by-component basis. This treatment essentially necessitated a distinction between two flavours of fragility curves: (a) an "individual" component fragility curve that

refers to the probability of exceeding the capacity of a specific (acceleration-sensitive) component given the IM and (b) a "combined" component fragility curve that denotes the probability of exceeding the capacity of any component of a specific IC in the building (see Table 1) given the IM. The latter condition in fact signals the transition of the entire asset to a specific DS due to nonstructural damage in the acceleration-sensitive equipment.

Both aleatory and epistemic uncertainties were considered. The record-to-record variability was accounted for via utilising the suite of the 30 ground motion records. Further to the above, with reference only to the acceleration-sensitive nonstructural components, the component amplification factor a_p, was also assumed to be lognormally distributed with a median per Kazantzi et al. (2020) and a dispersion equal to 0.30. The component acceleration capacity $S_{a_{cap}}$ was assumed to be normally distributed, having a median value equal to that obtained from Eq. (1) and a coefficient of variation (CoV) equal to 0.20.

6. Seismic fragilities

6.1. Drift-sensitive structural and nonstructural seismic fragilities

A drift-sensitive component fragility depicts the probability of a building violating a specific IDR limit (see Table 2) that is likely to induce damages in its structural or in its drift-sensitive nonstructural components. As expected for well-designed, constructed, and maintained low-rise building-type refinery structures, the median of the fragilities was found to be over 2g for both of the considered IMs. Hence, they are inconsequential for the overall asset performance. On another note, the dispersion of the structural fragility was overall found to be higher when computed for $AvgS_a$ (0.49–0.56) compared to *PGA* (0.28–0.35). This can be attributed to the periods of 0.1–1.0sec assumed for $AvgS_a$, whereas the fundamental periods of the two considered buildings are in the range of ~0.1–0.2sec (Table 1). On the other hand, targeting a facility-wide application under a single IM, means that one may have to accept such larger dispersion as a compromise for using $AvgS_a$, allowing a better evaluation for other critical facilities, such as liquid-storage tanks (Bakalis et al, 2018).

6.2 Combined acceleration-sensitive component seismic fragilities

The combined acceleration-sensitive component fragility curves are evaluated for the considered assets. To provide a comparative sense of component damageability, indicative fragilities are also presented for the individual components. The individual fragility curves of the 13 components (see Table 1 and Fig. 1b) nested in the 2-storey RC building (RC2) are depicted in Fig. 2a,b for PGA and $AvgS_a$, respectively, computed separately for each one of the principal (x, y) axes to account for the different dynamic characteristics of building and equipment. There are four components at the ground level belonging to IC III, six at the first-floor belonging to all three ICs, and another three at the roof level belonging to IC II and III. The weakest (and consequently most critical) components for IC I are the first-floor vessels in the x-direction (see Fig. 1b), for IC II the roof-level horizontal vessel in the y-direction, and for IC III a roof-level heat exchanger in the y-direction.

The median and the dispersion of the weakest individual component fragilities presented in Fig. 2 are also summarised in Table 3. Interestingly, it was found that the failure of the weakest component belonging to IC III occurs prior to the failure of the other components belonging to ICs that are paired with less severe DSs (Table 2). Hence, for the RC2 asset, DS3 will be the most critical, not only because its attainment denotes more severe damageable consequences for the building but also because it occurs at lower IM levels

compared to the less severe DSs. This observation is by no means unusual and it holds for both buildings. From a practical point of view, to improve the seismic performance of such assets, one may consider strengthening the anchorage of the critical IC III components or consider repositioning (if possible) such vulnerable equipment.

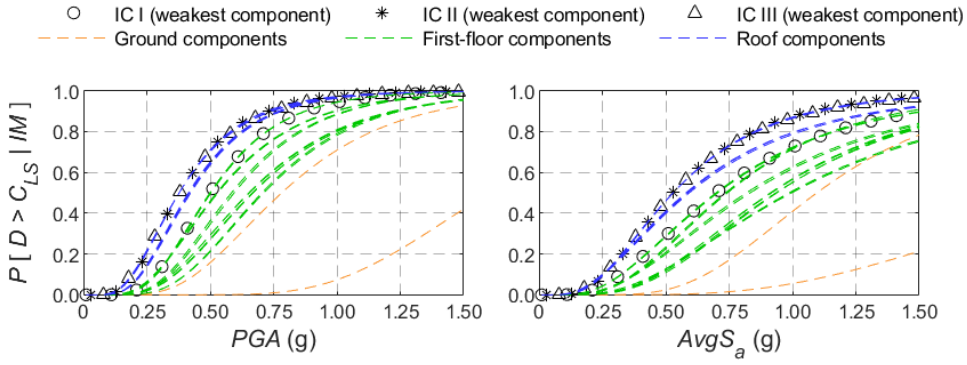

(a) (b)

Fig. 2 - Individual component fragility curves for the RC2 nested nonstructural acceleration-sensitive components for (a) PGA and (b) $AvgS_a$. The critical component for each IC is shown with markers.

Table 3. Median and dispersion of the individual component fragilities for the critical component of each IC (RC2 building).

Weakest component per IC	PGA		$AvgS_a$	
	median (g)	**dispersion**	**median (g)**	**dispersion**
IC I: First-floor vessel (x direction)	0.50	0.44	0.70	0.60
IC II: Roof horizontal vessel (y direction)	0.38	0.51	0.53	0.56
IC III: Roof heat exchanger (y direction)	0.38	0.53	0.53	0.58

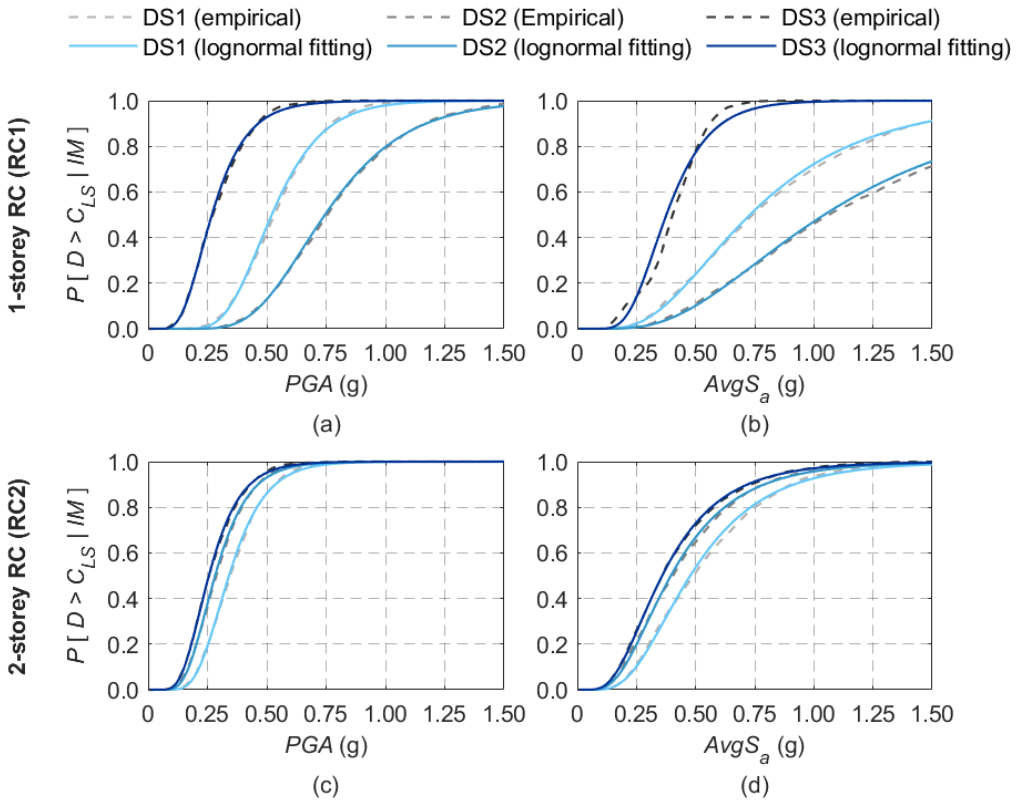

Fig. 3 - Combined component fragility curves for the (a-b) RC1 and (c-d) RC2 buildings.

Fig. 3 presents the empirical and the lognormally fitted combined component fragility curves for for both the considered buildings, whereas the combined fragility medians and dispersions are listed in Table 4. In all cases, the evaluation of the fragilities by simultaneously checking across components of the same IC for failure events, results in the fragilities being shifted to the left and to the dispersion being reduced, as opposed to the median and the dispersions that would have been obtained if the overall fragility was set equal to the fragility of the most critical component from each IC. Furthermore, as can be inferred from the results tabulated in Table 4, the attainment of the most severe DS3 occurs prior to DS1–2. This is simply a testament to the existence in each building of vulnerable, IC III equipment items that lead to early failures. Furthermore, among the two considered buildings, the most vulnerable is RC2. This is due to higher number of the above-ground critical components having periods very close to the fundamental periods of the supporting structure (0.20-0.21sec), a condition that essentially implies (near) tuning for these acceleration-sensitive components located at the first-floor and the roof and, consequently, high PCA demands.

Table 4. Median and dispersion of the combined component fragilities for each building

Building	Damage States	PGA		$AvgS_a$	
		median (g)	dispersion	median (g)	dispersion
1-storey RC (RC1)	**DS1**	0.52	0.32	0.73	0.53
	DS2	0.75	0.35	1.04	0.58
	DS3	0.27	0.43	0.38	0.38
2-storey RC (RC2)	**DS1**	0.34	0.35	0.48	0.51
	DS2	0.28	0.39	0.40	0.54
	DS3	0.26	0.40	0.36	0.54

7. Conclusions

A methodology is proposed for evaluating analytical fragility curves of equipment-supporting industrial buildings, in a way that can be readily integrated into the seismic risk assessment of an entire industrial plant. It was showcased that the seismic fragility of the nested acceleration-sensitive equipment is the one driving the overall seismic performance of such assets. The resulting models, data, and framework can be exploited for managing the seismic risk in such critical infrastructure.

Acknowledgements

The financial support provided by European Union through the Horizon 2020 research and innovation programmes “INFRASTRESS–Improving resilience of sensitive industrial plants & infrastructures exposed to cyber-physical threats, by means of an open testbed stress-testing system” under Grant Agreement No. 833088, and “HYPERION–Development of a decision support system for improved resilience & sustainable reconstruction of historic areas to cope with climate change & extreme events based on novel sensors and modelling tools” under Grant Agreement No. 821054 is greatly acknowledged. Thanks also go to Ms. E. Vourlakou for preparing the photorealistic images of the buildings.

References

- Bakalis K, Kohrangi M, Vamvatsikos D (2018) Seismic intensity measures for above-ground liquid storage tanks. Earthquake Engineering and Structural Dynamics 47(9): 1844–1863 https://doi.org/10.1002/eqe.3043

- Bakalis K, Vamvatsikos D, Fragiadakis M (2017) Seismic risk assessment of liquid storage tanks via a nonlinear surrogate model. Earthquake Engineering and Structural Dynamics 46(15): 2851–2868, https://doi.org/10.1002/eqe.2939
- CEN (European Committee for Standardization, 2004). Eurocode 8: Design of structures for earthquake resistance. Part 1: General rules, seismic actions and rules for buildings. EN1998-1. Brussels, Belgium, https://eurocodes.jrc.ec.europa.eu/showpage.php?id=138
- Cordova PP, Deierlein GG, Mehanny SS, Cornell CA (2000) Development of a two-parameter seismic intensity measure and probabilistic assessment procedure. Proceedings of the 2nd US–Japan Workshop on Performance-based Earthquake Engineering Methodology for RC Building Structures, Sapporo, Hokkaido.
- Cornell CA, Jalayer F, Hamburger RO, Foutch DA (2002) The probabilistic basis for the 2000 SAC/FEMA steel moment frame guidelines. Journal of Structural Engineering (ASCE) 128(4): 526–533, https://doi.org/10.1061/(ASCE)0733-9445(2002)128:4(526)
- Di Sarno L, Karagiannakis G (2020) On the seismic fragility of pipe rack–piping systems considering soil–structure interaction. Bulletin of Earthquake Engineering 18: 2723–2757, https://doi.org/10.1007/s10518-020-00797-0
- Dymiotis C, Kappos AJ, Chryssanthopoulos MK (1999) Seismic reliability of RC frames with uncertain drift and member capacity. Journal of Structural Engineering (ASCE) 125(9): 1038–1047, https://doi.org/10.1061/(ASCE)0733-9445(1999)125:9(1038)
- Eads L, Miranda E, Lignos DG (2015) Average spectral acceleration as an intensity measure for collapse risk assessment. Earthquake Engineering and Structural Dynamics 44(12): 2057–2073, https://doi.org/10.1002/eqe.2575
- Hatayama K (2008) Lessons from the 2003 Tokachi-oki, Japan, earthquake for prediction of long-period strong ground motions and sloshing damage to oil storage tanks. Journal of Seismology 12: 255–263, https://doi.org/10.1007/s10950-007-9066-y
- Kazantzi AK, Righiniotis TD, Chryssanthopoulos MK (2011) A simplified fragility methodology for regular steel MRFs. Journal of Earthquake Engineering 15(3): 390–403, https://doi.org/10.1080/13632469.2010.498559
- Kazantzi AK, Vamvatsikos D (2015) Intensity measure selection for vulnerability studies of building classes. Earthquake Engineering and Structural Dynamics 44(15): 2677–2694, https://doi.org/10.1002/eqe.2603
- Kazantzi AK, Vamvatsikos D, Miranda E (2020) Evaluation of seismic acceleration demands on building non-structural elements. Journal of Structural Engineering (ASCE) 146(7): 04020118, https://doi.org/10.1061/(ASCE)ST.1943-541X.0002676
- Kazantzi AK, Vamvatsikos D (2021) Practical performance-based design of friction pendulum bearings for a seismically isolated steel top story spanning two RC towers. Bulletin of Earthquake Engineering 19:1231-1248, https://doi.org/10.1007/s10518-020-01011-x
- Kiremidjian AS, Ortiz K, Nielsen R, Safavi B (1985) Seismic risk to major industrial facilities. Blume Earthquake Engineering Center, Report No. 72.
- Krausmann E, Cruz AM (2021) Natech risk management in Japan after Fukushima – What have we learned? Loss Prevention Bulletin, 277, https://www.icheme.org/media/15301/krausmannnew.pdf
- Lin T, Haselton CB, Baker JW (2013) Conditional spectrum-based ground motion selection. Part I: Hazard consistency for risk-based assessments. Earthquake Engineering and Structural Dynamics 42(12), 1847–1865, https://doi.org/10.1002/eqe.2301
- Kwon OS, Elnashai A (2006) The effect of material and ground motion uncertainty on the seismic vulnerability curves of RC structure. Engineering Structures, 28(2), 289–303, https://doi.org/10.1016/j.engstruct.2005.07.010
- McKenna F, Fenves GL (2001) The OpenSees Command Language Manual (1.2 edn). University of California Berkeley, Berkeley, CA.
- Patkas LA, Karamanos SA (2007) Variational solutions for externally induced sloshing in horizontal-cylindrical and spherical vessels. Journal of Engineering Mechanics (ASCE) 133(6): 641–655, https://doi.org/10.1061/(ASCE)0733-9399(2007)133:6(641)
- Tsantaki S, Adam C, Ibarra LF (2017) Intensity measures that reduce collapse capacity dispersion of P-delta vulnerable simple systems. Bulletin of Earthquake Engineering 15(3): 1085–109, https://doi.org/10.1007/s10518-016-9994-4
- Vathi M, Karamanos SA, Kapogiannis IA, Spiliopoulos KV (2017) Performance Criteria for Liquid Storage Tanks and Piping Systems Subjected to Seismic Loading. Journal of Pressure Vessel Technology (ASME) 139(5): 051801 https://doi.org/10.1115/1.4036916